Driver Drowsiness Detection Using R-R Interval of Electrocardiogram and Self-Attention Autoencoder

Koichi Fujiwara, *Member, IEEE*, Hiroki Iwamoto, Kentaro Hori, Manabu Kano, *Member, IEEE*

***Abstract*—Drowsy driving detection is crucial for avoiding serious traffic accidents. Changes in sleep conditions affect the autonomic nervous system (ANS) and, subsequently, heart rate variability (HRV), which is fluctuation in the R-R interval (RRI) in an electrocardiogram (ECG). HRV is easy to measure with a wearable sensor, and it may be possible to use HRV to detect drowsy driving. In conventional HRV-based drowsy driving detection methods, some HRV features are extracted from RRI data for analysis, but it may result in the loss of time-series characteristics of the RRI data. This study proposes a new driver drowsiness detection method that can detect abnormal changes in the RRI data caused by drowsiness. The proposed method employs a self-attention autoencoder (SA-AE), which is a type of neural network that can utilize time series characteristics. An experiment with a driving simulator was performed to evaluate the drowsiness detection performance of the proposed method. In this experiment, RRI data were collected from 20 participants (nonprofessional drivers) while driving, whose sleep conditions were scored by a sleep specialist based on electroencephalography (EEG) data. The experimental result showed that the proposed RRI-based drowsiness detection method detected 16 out of 18 sleep-related events while driving (sensitivity of 88 %), and a false-positive rate of 0.60 times per hour was achieved. In addition, we validated the proposed method employing 18 middle-aged professional drivers. The proposed drowsiness detection method would contribute to preventing accidents caused by drowsy driving in the future.**

***Index Terms*—Drowsy driving, Sleep scoring, R-R interval, Self-attention autoencoder, Electroencephalography**

I. Introduction

Drowsy driving is a major cause of fatal traffic accidents, with the risk of traffic accidents in drowsy driving estimated as being four to six times higher than in awake driving [1]. Detecting drivers' drowsiness and warning them are crucial for preventing accidents caused by drowsy driving.

Some conventional methods for detecting driver drowsiness have utilized electroencephalography (EEG) [2], [3]. Sleep stages are defined based on EEG in sleep medicine [4], and EEG recording is the gold standard method for sleep scoring. This fact has motivated some to try to use EEG for the purpose described above. However, EEG-based drowsiness detection methods are not always feasible because it is difficult to accurately record EEG while driving. In addition, EEG recording is intolerant to motion artifacts caused by driving operations, electromagnetic noise caused by onboard equipment and vibrations caused by the engine and the road surface during driving.

Images of drivers' faces and vehicle travel data have been used in place of EEG [5]–[7]. These methods, however, have the disadvantage that they require special equipment such as cameras and data logging devices.

Physiological signals, particularly cardiac signals, can be used for driver drowsiness detection because, as it is well-known, the autonomic nervous system (ANS) and cardiac activities are affected by sleep condition [8]. Chui *et al.* developed a driver drowsiness detection system using electrocardiogram (ECG) signals of drivers [9]. Photoplethysmography (PPG) signals have also been used for detecting drowsiness [10]. However, motion artifacts prevent stable measurement of ECG and PPG. In addition, ECG and PPG signal processing requires a heavy computational load because the required sampling rate is usually more than several hundred Hz, which also leads to shortened battery life.

Heart rate variability (HRV) is a well-known physiological phenomenon that reflects activities of ANS [11]. An ECG trace consists of some peaks, as shown in Fig. 1, the highest of which is an R wave. The R-R interval (RRI) [ms] is defined as the interval between an R wave and the next R wave. HRV is defined as the fluctuation in the RRI. HRV analysis has traditionally been employed in the cardiovascular field [12] and recently has been used for various types of health monitoring. An HRV-based epileptic seizure prediction system was developed and implemented as a wearable heart rate sensor and a smartphone app [13], [14]. Sleep apnea screening algorithms have been developed by monitoring HRV during sleep [15], [16].

HRV-based driver drowsiness detection methods have been proposed based on the fact that HRV is altered at the time of sleep stage transition [17]. Babaeian *et al.* proposed a

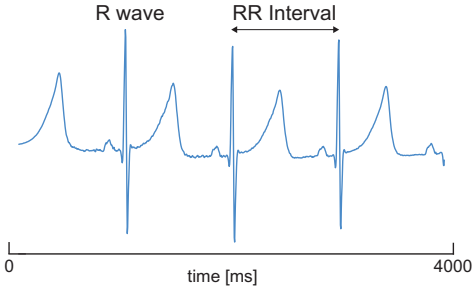

Fig. 1. Example of ECG trace (standard lead II).

Manuscript received May. xx, 2023; This work was partially supported by JSPS KAKENHI #21H03851.

K. Fujiwara is with the Department of Materials Process Engineering, Nagoya University, Nagoya, Japan, 464-8601 e-mail: fujiwara.koichi@hps.material.material-u.ac.jp.

H. Iwamoto, K. Hori, and M. Kano are with Kyoto University.

drowsiness detection method combining HRV analysis and wavelet analysis [18]. They specified characteristic changes in HRV around drowsiness with continuous wavelet transform (CWT), and the features extracted by CWT were discriminated whether drivers feel drowsy or not with an ensemble logistic regression model. A drowsiness detection model using the frequency-domain features of HRV was developed with linear discriminant analysis [19]. Focusing on the relationship between traffic accidents and fatigue or drowsiness of drivers, Ito *et al.* developed a model for evaluating a future collision risk based on HRV [20]. On the other hand, Fujiwara *et al.* proposed an HRV-based driver drowsiness detection method using an anomaly detection approach because collecting the drowsy driving data is more difficult than the awake driving data [21].

The use of HRV for drowsy driving detection may be feasible since R wave detection and HRV analysis are much more robust against artifacts than EEG, even in a vehicle, because the amplitude of R waves in ECG signals is much higher than in EEG signals. Additionally, ECG is easy to measure using a simple wearable sensor. Since an R wave in an ECG signal occurs every second, the processing load thereof is much lighter than that of the ECG and PPG-based methods, which require heavy signal processing. Thus, HRV-based methods can reduce energy consumption when implemented in mobile computers such as smartphones.

HRV feature extraction, however, may cause a loss of important time information in the RRI data because it uses a window function to clip the RRI data for several minutes. Since falling asleep is an instantaneous event, standard HRV features might not detect such events. Raw RRI data that retain time information should be employed for drowsy driving detection as an alternative to HRV features because RRI data may retain time information of short-duration events. Iwasaki *et al.* showed that the use of raw RRI data improved the performance of a screening algorithm for sleep apnea, which is also an instantaneous event like falling asleep, in comparison with HRV features [16].

A new driver drowsiness detection method based on anomaly detection is proposed in the present work. In the proposed method, raw RRI data are utilized instead of HRV features. The proposed method uses a self-attention autoencoder (SA-AE) as an anomaly detection algorithm, which consists of a self-attention mechanism for sequence data analysis [22], and an autoencoder, which is a type of neural network for representation learning and anomaly detection [23]. In order to appropriately consider the time-series characteristics of the RRI data, the SA mechanism is employed. In the proposed method, abnormal changes in the RRI data due to drowsiness during driving are detected with SA-AE. An experiment using a driving simulator was performed to evaluate the drowsiness detection performance of the proposed method.

A preliminary version of this work has been described in [24], but this report did not include the SA-AE model.

II. Definition and Scoring of Drowsiness

According to somnology, sleep consists of rapid eye movement sleep (REM) and non-REM sleep (NREM), the latter of which is broken down into three stages: N1, N2, and N3 [4]. N1 usually occurs between wakefulness and deeper sleep. During N1, muscles are still active, and eyelids may open and close moderately frequently. Thus, people in N1 can be easily awakened by means of sensory stimuli. Fujiwara *et al.* have reported that they were able to detect N1 onsets by monitoring HRV [21]; however, other sleep-related events should be considered in addition to N1 onsets in order to detect drowsiness.

Slow eye movements (SEM) are often observed in the transitional period from awake to N1 [25]. Microsleep is a sudden, short sleep lasting for a fraction of a second or up to a few seconds and is a well-known phenomenon in sleep science [26]. People experiencing microsleep often remain unaware of them. The occurrence of microsleep becomes dangerous, particularly in situations that demand constant alertness, such as driving or working with heavy machinery.

N1 onsets, SEMs, and microsleeps of the driver should be detected because he/she can be easily awakened at the time of these events by means of a light stimulus, which could prevent accidents.

Sleep stages and sleep-related events are defined based on EEG and electrooculogram (EOG) in somnology [27]. N1 onset (sleep onset) is defined by the epoch in which α wave (8-13Hz) activity is attenuated and replaced by low-amplitude, mixed-frequency activities that occupy more than 50% of a 30-second epoch. SEM can be labeled based on EOG. Microsleep is identified as a short awake α wave appearance on EEG in this study. Since these sleep-related events cannot be visually scored based on facial images of drivers, this study employed the EEG scoring method used in somnology [27].

Jurysta *et al.* have reported that cardiac activities precede EEG changes relating to sleep stage transition by 9–20 minutes (mean 12 minutes) [28]. In addition, there is some uncertainty in the detection timing of sleep-related events even among well-trained experts [29]. Based on these prior reports, "drowsy" is defined in this study as a period from fifteen minutes before to three minutes after a sleep-related event occurrence, and the remaining period is defined as "awake".

III. Drowsy Driving Detection

This work proposes a new drowsiness detection method based on a framework for detecting anomalies in RRI data of drivers.

A. Anomaly Detection in RRI Data

Standard binary classification algorithms require almost the same number of positive and negative samples. Collecting sufficient negative (abnormal) samples is sometimes difficult while collecting positive (normal) samples is much easier. In this case, a model should be trained using normal samples only, and samples that have different characteristics from the normal data are detected as abnormal samples with the trained model. This framework is called anomaly detection in machine learning. Driver drowsiness detection is formulated as anomaly detection because it is much easier to collect awake driving data than drowsy driving data from drivers.

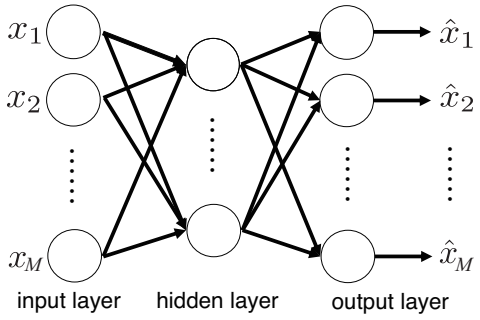

Fig. 2. Structure of AE.

Fujiwara *et al.* proposed a driver drowsiness detection method combining HRV analysis and multivariate statistical process control (MSPC) [21], [30] which is a well-known anomaly detection algorithm used in industrial process monitoring [31], [32] as well as health monitoring [13], [33]. MSPC is a linear anomaly detection method because it is based on principal component analysis (PCA). Although it is difficult for MSPC to deal with nonlinearity, HRV is a nonlinear phenomenon [34]. Hence, nonlinear anomaly detection algorithms should be used.

An autoencoder (AE) is a neural network model that is trained so that the outputs become close to the inputs [23]. A structure of an AE is illustrated in Fig 2. An AE model consists of an input layer, a hidden layer, and an output layer. $x_1, \cdots, x_M$ and $\hat{x}_1, \cdots, \hat{x}_M$ are the input variables and the output variables of the AE model, respectively. In Fig 2, circles denote units that express activation functions. The AE is interpreted as a nonlinear expansion of PCA because the AE model becomes PCA when all of the activation functions in hidden layers are the identity function [35].

AE can also be used for anomaly detection [36]. It is assumed that an AE is trained with normal data only. Reconstruction error (RE), which is the error between the input and the output of the AE model, is small when the input is a normal sample; on the other hand, RE becomes large when an abnormal sample is input to the AE model. Since AE can cope with nonlinearity, it may be more suitable than MSPC for anomaly detection in RRI data. Thus, this work employs AE for drowsy driving detection.

In addition, the time-series characteristics of the RRI data should be taken into account. A self-attention (SA) network [22], [37] is a type of neural network that can handle time-series data with an attention mechanism. The SA network can be combined with the AE for anomaly detection of time-series data. This network architecture is referred to as SA-AE.

A graphical summary of the drowsiness detection model with SA-AE is shown in Fig. 3. The input RRI data $\boldsymbol{y} \in \mathbb{R}^L$ is expanded to multi-dimensional data by a first fully connected layer (FC), and features are extracted in hidden layers from the expanded multi-dimensional data with multi-head SA and the FC. L is the length of the RRI data. The colored block in Fig. 3 is stacked multiple times. Each block has a skip connection that is expected to promote training [38]. The output of the last FC is the output RRI data $\hat{\boldsymbol{y}} \in \mathbb{R}^L$.

An SA-AE model for anomaly detection is trained from the RRI data of drivers collected during awake driving. The RE stays small when the input is an awake RRI, and the RE becomes large when a drowsy RRI is input to the trained SA-AE model. The RE is defined as

$$\mathrm{RE} = \|\boldsymbol{y} - \hat{\boldsymbol{y}}\|^2 = \sum_{l=1}^{L} (y_l - \hat{y}_l)^2. \tag{1}$$

Driver drowsiness is detected when RE exceeds a predefined threshold $\overline{\mathrm{RE}}$.

B. Model Training

Before using the proposed method, a drowsiness detection SA-AE model must be trained with the RRI data of drivers collected during awake driving. A model training procedure is described in Algorithm 1.

The RRI data collected from the ith driver $(i = 1, \ldots, I)$ is denoted as

$$\boldsymbol{y}^{[i]} = \left[r_1^{[i]},\ r_2^{[i]},\ \cdots,\ r_j^{[i]}, \cdots,\ r_{L_i}^{[i]} \right] \in \mathbb{R}^{L_i} \tag{2}$$

where $r_j^{[i]}$ is the jth RRI measurement of the ith driver, and L_i is the length of $\boldsymbol{y}^{[i]}$. In step 2, the ith RRI data $\boldsymbol{y}^{[i]}$ is arranged in an RRI data matrix $\boldsymbol{Y}^{[i]} \in \mathbb{R}^{(L_i - M + 1) \times M}$ as follows:

$$\boldsymbol{Y}^{[i]} = \begin{bmatrix} r_1^{[i]} & r_2^{[i]} & \cdots & r_M^{[i]} \\ r_2^{[i]} & r_3^{[i]} & \cdots & r_{M+1}^{[i]} \\ \vdots & \vdots & \vdots & \vdots \\ r_{L_i-M+1}^{[i]} & r_{L_i-M+2}^{[i]} & \cdots & r_{L_i}^{[i]} \end{bmatrix} \tag{3}$$

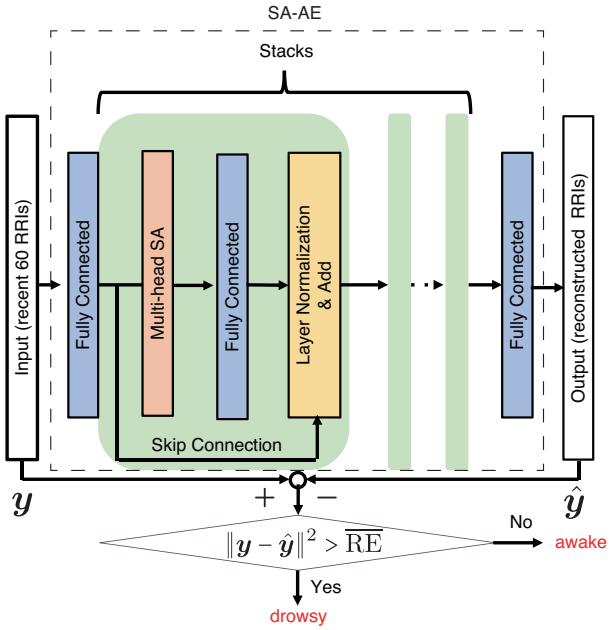

Fig. 3. Schematic diagram of drowsiness detection model

L is the length of input of SA-AE. $\boldsymbol{Y}^{[1]}, \cdots, \boldsymbol{Y}^{[I]}$ is merged into one matrix $\boldsymbol{Y} \in \mathbb{R}^{L \times M}$ in step 4

$$\boldsymbol{Y} = \begin{bmatrix} \boldsymbol{Y}^{[1]} \\ \boldsymbol{Y}^{[2]} \\ \vdots \\ \boldsymbol{Y}^{[I]} \end{bmatrix}. \tag{4}$$

In step 5, the merged matrix $\boldsymbol{Y}$ is normalized to zero mean and unit variance, which is denoted as $\tilde{\boldsymbol{Y}}$. Finally, a drowsiness detection SA-AE model f is trained from $\tilde{\boldsymbol{Y}}$ in step 6.

C. Drowsiness Detection

The proposed method detects driver drowsiness using the drowsiness detection model f trained in Algorithm 1. f estimates the driver condition as a binary state $S \in \{\mathcal{A}, \mathcal{D}\}$, which denotes 'awake' and 'drowsy' respectively, and $\neg\mathcal{A} = \mathcal{D}$ and vice versa.

Before driver drowsiness detection starts, the initial RRI data must be stored for more than the length of the RRI data L in the SA-AE model. After the initial RRI data collection, driver drowsiness is monitored by following Algorithm 2. $y[t] \in \Re$ denotes the tth RRI where t is the number of samples taken from the start of driver drowsiness detection. τ is a time counter variable.

Because RE may fluctuate due to RRI artifacts, the driver status is determined in this algorithm as 'drowsy' only when RE continuously exceeds its threshold $\overline{\mathrm{RE}}$ for more than the predefined period $\bar{\tau}$. Conversely, driver status transitions from 'drowsy' to 'awake' when RE continuously stays below its threshold $\overline{\mathrm{RE}}$ for more than $\bar{\tau}$.

The threshold $\overline{\mathrm{RE}} = \max\{\overline{\mathrm{RE}}_0, \overline{\mathrm{RE}}'\}$ is adopted in this study, where $\overline{\mathrm{RE}}_0$ is a shared default threshold and $\overline{\mathrm{RE}}'$ is an individual threshold to consider individual differences in the RRI data of drivers. The individual threshold $\overline{\mathrm{RE}}'$ can be tuned for each driver using the $\alpha\%$ confidence limit of the RE, calculated based on the awake part of the RRI data of each driver; in other words, $\overline{\mathrm{RE}}'$ is set so that $\alpha\%$ of the RRI data representing the awake condition is below, and the other $(100-\alpha)\%$ is above, $\overline{\mathrm{RE}}$.

IV. Experiment

This section reports the results of applying the proposed drowsy driving detection method to experimental data.

Algorithm 1 Drowsiness Detection Model Training

Require: The RRI data of $\{\boldsymbol{y}^{[1]}, \boldsymbol{y}^{[2]}, \cdots, \boldsymbol{y}^{[I]}\}$.
1: **for** $i = 1, \ldots, I$ **do**
2: Rearrange $\boldsymbol{y}^{[i]}$ to $\boldsymbol{Y}^{[i]}$.
3: **end for**
4: Merge $\boldsymbol{Y}^{[i]}$ $(i = 1, \ldots, I)$ into one matrix $\boldsymbol{Y}$.
5: Normalize $\boldsymbol{Y}$, which is referred to as $\tilde{\boldsymbol{Y}}$.
6: Train the SA-AE model f from $\tilde{\boldsymbol{Y}}$.
7: **return** The trained f.

Algorithm 2 Drowsiness Detection

Require: The trained drowsiness detection model f.
$S[0] \longleftarrow \mathcal{A}$ and $\tau[0] \longleftarrow 0$.
while **do**
Collect the newly measured tth RRI $y[t]$.
Construct the ith input $\boldsymbol{y}[t] = [y[t-M+1], \ldots, y[t]]$.
Normalize $\boldsymbol{y}[t]$, which is referred to as $\tilde{\boldsymbol{y}}[t]$.
Calculate the tth output $\hat{\boldsymbol{y}}[t]$ by inputting $\tilde{\boldsymbol{y}}[t]$ into the drowsiness detection model f.
Calculate the tth RE $E[t]$ between $\tilde{\boldsymbol{y}}[t]$ and $\hat{\boldsymbol{y}}[t]$.
if $((RE[t] > \bar{RE}) \wedge (S = \mathcal{A})) \vee ((E[t] \leq \bar{E}) \wedge (S = \mathcal{D}))$ **then**
$\tau[t] \longleftarrow \tau[t-1] + y_i$
else
$\tau[t] \longleftarrow 0$
end if
if $\tau[t] \geq \bar{\tau}$ **then**
$S[t] \longleftarrow \neg S[t-1]$ and $\tau[t] \longleftarrow 0$.
end if
Wait until the next RRI $y[t+1]$ is measured.
end while

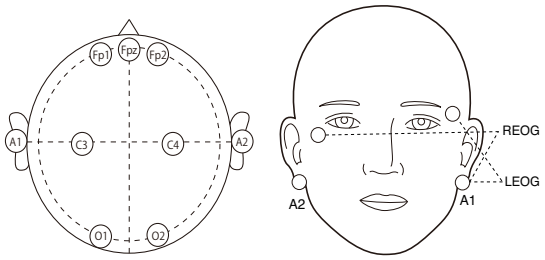

Fig. 4. Electrode allocations for sleep scoring: EEG (left) and EOG (left)

A. Data Collection with Nonprofessional Drivers

The RRI and EEG data were collected from experiment participants (drivers) while they drove a virtual vehicle on a simulator. Although 31 persons participated in the experiment, data collected from 11 participants were excluded due to measurement failure or inappropriate health conditions. The remaining 20 participants (male: 13, female: 7, 21.2±1.9 years old) were used for analysis. The inclusion criteria for the participants were nonprofessional drivers with valid driving licenses. The exclusion criterion was having a confirmed diagnosis of a chronic illness that may affect ECG, such as cardiovascular disease, arrhythmia, epilepsy, or sleep disorders. In addition, participants were asked to answer the Japanese version of the Epworth sleepiness scale (ESS) [39] and the patient health questionnaire 9 (PHQ-9) in order to assess the participants' daily sleepiness and mental conditions [40]. This experiment and analysis were approved by the Research Ethics Committee of the Graduate School of Informatics, Kyoto University. Written informed consent was obtained from each participant prior to the experiment.

The utilized driving simulator (DS) is the UC-win/road system (FORUM8 Co. Ltd., Japan), which consists of a PC, a steering wheel, a driving seat, and four LCD monitors (three for the front scene and one for the instrument panel).

Fig. 5. Example of experimental scene.

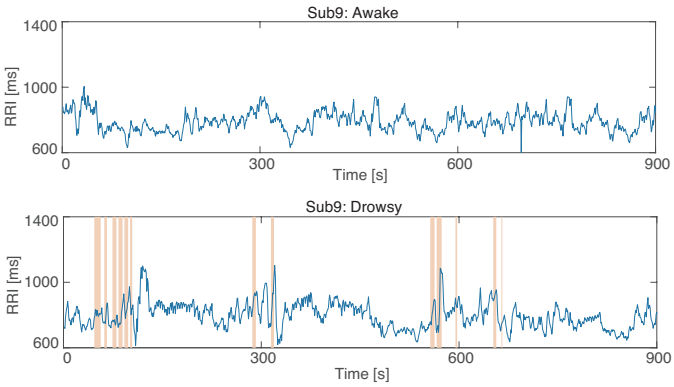

Fig. 7. RRI collected from participant N9: awake period (top) and drowsy period (bottom)

To induce driver drowsiness, the experiment was performed in a dark room, and the room air temperature was maintained around 25 °C. The participants drove along a monotonous circuit course consisting of long straight roads and gentle curves for about three hours, and no extra tasks were not assigned during driving. Although the maximum speed of the virtual vehicle is 140 km/h, they were asked to maintain a speed between 60 and 80 km/h. Simulated vehicle cruise sounds and environmental sounds were played from speakers of the DS; however, any music was not played during driving. Each participant performed driving once. Figure 5 shows an example of an experimental scene.

ECG, EEG, and EOG during driving were measured with the Grapevine Neural Interface Processor system (Ripple Neuro inc., USA), with a sampling frequency of 1,000 Hz. Although the International 10-20 system is a standard scalp electrode allocation of EEG recording, a reduced electrode allocation was employed, as shown in Fig. 4 (left) because this allocation is sufficient for sleep scoring. Fp1, Fp2, C3, C4, O1, and O2 were EEG electrodes, earlobes A1 and A2 were for reference, and Fpz was the body earth. EOG was recorded during driving for SEM detection. The EOG electrode allocation is shown in Fig. 4 (right), wherein the left earlobe A1 was used for reference.

Figure 6 is an example of the ECG data of 60 beats during the awake period measured by participant N9, which shows that the quality of the ECG data measured in this experiment was sufficiently high.

Since motion artifacts were generated when participants moved during driving, data in which the EEG data were contaminated with strong artifacts were eliminated before analysis. Based on the collected EEG and EOG data, a sleep specialist certificated by the Japanese Society of Sleep Research scored sleep-related events–N1 onsets, microsleeps, and SEM–in accordance with the standard sleep scoring method in somnology [27]. Based on the definition of drowsy described in Sec. II, nine participants had a total of 30 sleep-related events during driving.

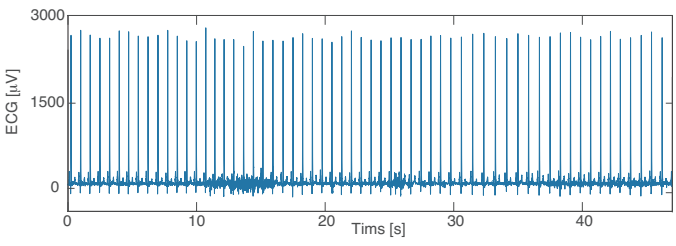

Fig. 6. ECG measured from participant 9

B. Data Preprocessing

The participants were divided into three groups in accordance with the results of sleep scoring: training, validation, and test groups for machine learning.

Drowsy RRI data are not needed in the training phase of a drowsy detection model because the training of SA-AE only requires normal (awake) data. The validation group was used for hyperparameter tuning of the model so that a good balance between sensitivity and specificity could be achieved. The drowsiness detection performance of the trained model was assessed with the test group. An overview of the data used for analysis is shown in Table I. In the table, 'W' and 'W/O' denote the numbers of participants with and without sleep-related events, respectively, and '#events' means the number of sleep-related events in each group.

The R waves were detected from the ECG data collected during driving using a first derivative-based peak detection algorithm, and the RRIs were calculated. Figures 7 and 8 illustrate examples of awake and drowsy RRI data collected from participants N9 and N28. Orange-colored bands denote the sleep-related events scored by the sleep specialist. These figures show that it is difficult to detect drowsiness through visual monitoring of the RRI data and, thus, that machine learning techniques should be used.

TABLE I
DATASET PROFILE (NONPROFESSIONAL DRIVERS)

	W/O	W	#events	Awake [h]	Drowsy [h]
Training	7	0	0	6.6	–
Validation	3	3	7	7.8	1.7
Test	2	5	18	5.0	4.7
Total	12	15	30	19.4	6.4

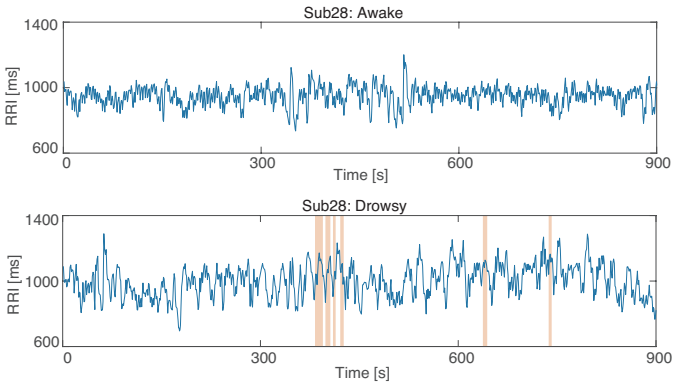

Fig. 8. RRI collected from participant N28: awake period (top) and drowsy period (bottom)

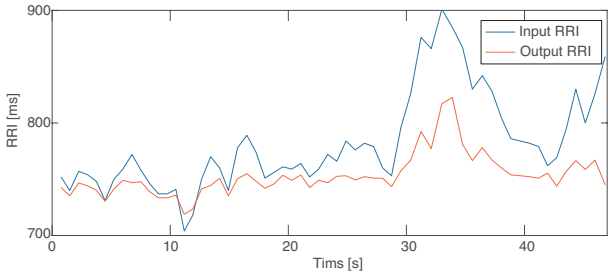

Fig. 9. Input and output RRI data with the SA-AE model of participant N9

C. Model Training

An SA-AE model was trained with the training data. The activation function in the FC was the rectified linear units (ReLU), and the input length of the RRI data L was determined as $L = 60$ in accordance with [16]. The adaptive moment estimation (Adam) was used as the optimizer. The hyperparameters of SA-AE were tuned with the Bayesian optimization using the validation data. In Algorithm 1, $\bar{\tau} = 7$ was determined, which was also determined by the Bayesian optimization.

With regard to the threshold $\overline{\mathrm{RE}}$, the shared default threshold $\overline{\mathrm{RE}}_0$ was determined with the validation data to be $\overline{\mathrm{RE}}_0 = 27$. In addition, the individual threshold was tuned with the 99% confidence limit of the awake RRI data of each driver. The 99% confidence is a standard setting of anomaly detection [13].

D. Results

The sleep-related events, the N1 onset, SEM, and microsleep in the validation data of eight participants were detected as driver drowsiness following Algorithm 2.

Figure 9 illustrates an example of the input and the output RRI data with the trained SA-AE model of participant N9, whose period corresponds to the ECG data shown in Fig. 6. This figure shows the output data of the trained SA-AE model followed the trend of the input data, although there were some errors. Thus, it is concluded that the trained model functioned successfully.

The drowsiness detection results of participants N9 and N28 are shown in Figs. 10 and 11. Orange and blue colored bands

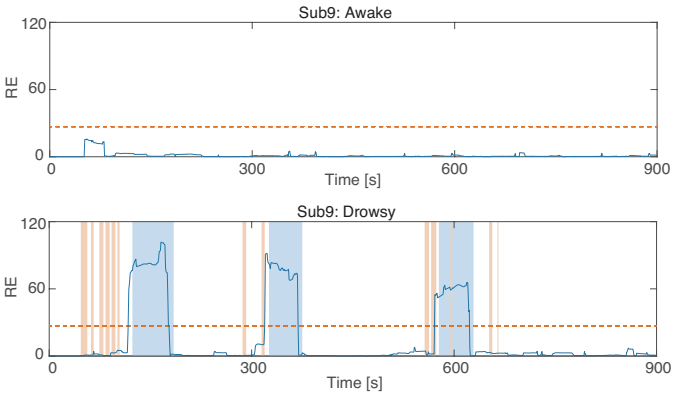

Fig. 10. Drowsiness detection results of participant N9: awake period (top) and drowsy period (bottom)

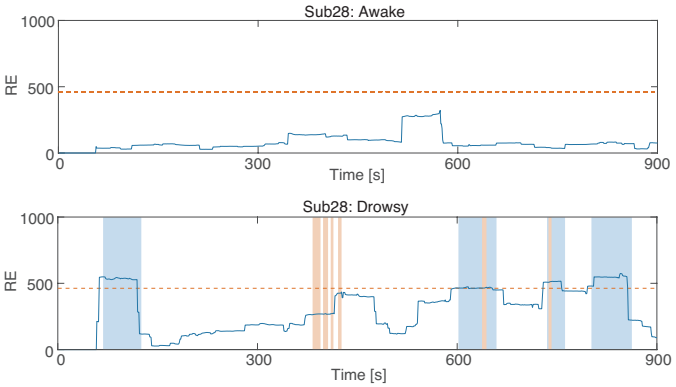

Fig. 11. Drowsiness detection results of participant N28: awake period (top) and drowsy period (bottom)

denote the sleep-related events scored by the sleep specialist and drowsiness detection periods according to the trained drowsiness detection model. These figures show that the drowsiness detection model detected driver drowsiness around occurrences of the sleep-related event, and false positives (FPs) rarely occurred.

The results of each participant are listed in Table II. The drowsiness detection model detected 16 out of 18 sleep-related events; that is, the sensitivity was 89%. In addition, only three FPs occurred in the awake periods (a total of 5.0 hours), and the FP rate was 0.60 times per hour.

TABLE II
DROWSINESS DETECTION RESULT (NONPROFESSIONAL DRIVER)

Participant	Sensitivity [%]*	FP rate [times/h]
N9	50 (2/4)	0.00
N12	100 (2/2)	0.00
N24	100 (5/5)	0.00
N27	- (0/0)	0.00
N28	100 (1/1)	0.61
N30	100 (6/6)	0.00
N31	- (0/0)	1.27
Total	89 (16/18)	0.59

* Parentheses denote the numbers of detected sleep-related events and occurring sleep-related events.

E. Additional Experiment with Professional Drivers

In order to validate the proposed drowsiness detection method, an experiment with 18 middle-aged professional bus drivers (male: 18, female: 0, 49.3±7.7 years old) was performed in addition to the experiment with the young participants. The exclusion criterion was having a confirmed diagnosis of a chronic illness that may affect ECG, such as cardiovascular disease, arrhythmia, epilepsy, or sleep disorders. The participants were all middle-aged males, reflecting the employment trend in Japan.

The experiment and model training were conducted following the same procedures described in Secs IV-A - IV-C. In this additional experiment, a model was newly trained for professional drivers because the physiological characteristics between professional and nonprofessional drivers were significantly different. Table III shows an overview of the data used for analysis.

Table IV lists the drowsiness detection results of each participant. The trained model detected 9 out of 10 sleep-related events; that is, the sensitivity was 90%. On the other hand, 11 FPs occurred in the awake periods (a total of 5.8 hours), meaning the FP rate was 1.90 times per hour. Thus, more FPs occurred in professional drivers than in nonprofessional drivers, while the sensitivity was the same.

V. Discussion

In the experiment with the nonprofessional drivers, 16 out of 28 sleep-related events were detected with the drowsiness detection model; however, two out of four sleep-related events in participant N9 were not detected. Figure 12 shows the RRI data and RE around the sleep-related event of participants 9 that were not detected by the drowsiness detection model.

The sleep-related events of participant N9 were all SEMs, and the duration of SEM in Fig. 12 was very short (about 3 seconds). These points suggest that it is more difficult to detect short SEM than N1 onsets and microsleep from the RRI data.

On the other hand, three FPs occurred in the awake periods. One FP was in participant 28, and two were in participant N31. It is confirmed that their RRI data did not contain any artifacts due to ECG electrode contact failure or arrhythmia. The ESS scores of participants N28 and N31 were 14 and 8, respectively, which indicates that participant N28 had mild sleepiness while participant N31 was healthy because the cutoff value of the ESS score is usually 11 [41]. The causes of the FPs of participant N31 are unknown.

TABLE III
Dataset profile (professional drivers)

	W/O	W	#events	Awake [h]	Drowsy [h]
Training	6	0	0	5.7	–
Validation	4	2	9	2.4	2.5
Test	2	3	11	5.2	3.0
Total	13	5	20	13.3	5.5

TABLE IV
Drowsiness detection result (professional driver)

subject	Sensitivity [%]*	FP rate [times/h]
P2	100 (1/1)	2.02
P9	- (0/0)	0.00
P16	- (0/0)	0.00
P21	100 (8/8)	16.0
P22	0 (0/1)	0.00
Total	90 (9/10)	1.90

* Parentheses denote the numbers of detected sleep-related events and occurring sleep-related events.

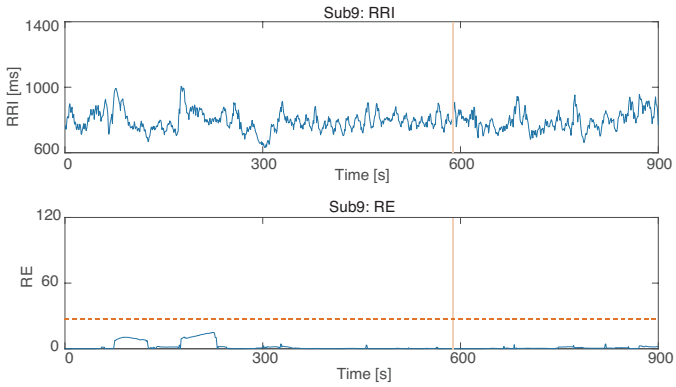

Fig. 12. RRI data (top) and RE (bottom) around the sleep-related event of participants 9

In this study, the threshold RE varied depending on each participant because the individual threshold $\overline{\mathrm{RE}}'$ was used instead of the shared default threshold $\overline{\mathrm{RE}}_0$ when $\overline{\mathrm{RE}}' > \overline{\mathrm{RE}}_0$. In order to verify this setting, we checked the performance of the drowsiness detection algorithm so that the threshold RE was defined as the shared default threshold $\overline{\mathrm{RE}}_0$ or the individual threshold $\overline{\mathrm{RE}}'$ only. The sensitivity and the FP rate were 70% and 1.60 times/hour, respectively when $\overline{\mathrm{RE}}_0$ was adopted, and the use of $\overline{\mathrm{RE}}'$ achieved a sensitivity of 100% and the FP rate of 6.6 times/hour. These results suggest that the combination of $\overline{\mathrm{RE}}'$ and $\overline{\mathrm{RE}}_0$ was effective for achieving a well-balanced performance that can deal with individual differences in the RRI data collected from drivers.

The self-attention (SA) network is employed in order to take the time-series characteristics of the RRI data into account. Other types of networks have been proposed to handle time-series data, long short-term memory (LSTM) being one such network [42]. LSTM autoencoder (LSTM-AE) was tried as the drowsiness detection model to compare with SA-AE. The LSTM-AE model detected 12 out of 18 sleep-related events (sensitivity of 67%), and the FP rate was 0.4 times/hour. Thus, the sensitivity of the LSTM-AE model was inferior to that of the proposed SA-AE model, while its FP rate was better than that of the SA-AE model. From the viewpoint of preventing accidents caused by drowsy driving, the SA-AE model is preferable to the LSTM-AE model; however, further performance improvements of the LSTM-AE model may be achieved when appropriate hyperparameters are found.

Iwasaki *et al.* developed an RRI-based sleep apnea screening model, whose length of input RRI data is 60 [16]. Based on their study, $L = 60$ was also employed as the length of input RRI data in the drowsiness detection model. In order to investigate the effect of L on the drowsiness detection performance, other lengths of the input RRI data were tested

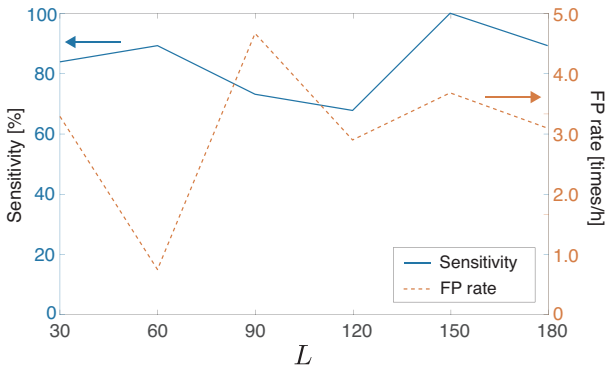

Fig. 13. Sensitivities and FP rates with $L = 30, 60, 90, 120, 150, 180$

in addition to the original $L = 60$: 30, 90, 120, 150, and 180. Figure 13 shows changes in the sensitivities and the FP rates. A sensitivity of 100% was achieved when $L = 150$; however, its FP rate was more than three times/hour, and the FP rate was best when $L = 60$. Considering the balance between the sensitivity and the FP rate, RRI vectors with $L = 60$ were appropriate.

The additional experiment employing the professional drivers was conducted to validate the proposed method, which shows that many FPs occurred while the sensitivity did not deteriorate in comparison with the nonprofessional drivers. The age of the professional drivers was higher than that of nonprofessional ones. The prevalence of sleep disorders, such as sleep apnea and insomnia, or cardiovascular diseases like arrhythmia increases with age [43], [44]. These disorders significantly affect ANS and cardiac activities [45], which might increase FP occurrences in nonprofessional drivers. According to Table IV, participant P21 (44 years old), who had many sleep-related events, also had many FPs. This indicates that he might have an unconfirmed and unaware sleep disorder. According to a report from the US, about 80% of patients with apnea remain undiagnosed and untreated [46]. Thus, it may become difficult to detect drowsiness for middle or older-aged participants.

In this study, two different drowsiness detection models were trained for professional and nonprofessional drivers, respectively, by considering the difference in physiological characteristics. When a model was trained from the data consisting of both professional and nonprofessional drivers, its sensitivity and the FP rate were 62% and 3.2 times per hour. This result suggests that the drowsiness detection model should be trained by each age group.

In order to use the conventional HRV-based drowsiness detection methods, drivers need to wait at least two minutes before the start of operation since calculating HRV indexes requires at least two minutes of RRI data according to the clinical guideline of HRV analysis [47]. Fujiwara *et al.* used three minutes of RRI data for HRV analysis. The latency time of their method is three minutes [21]. In the proposed method, drivers also must wait until the initial RRI data are stored. The input of the proposed method is the RRI data with $L = 60$, which can be converted to about a one-minute duration because one RRI (one beat-to-beat interval) is almost one second. Hence, the latency time of the proposed method is about one minute, which is shorter than the HRV-based methods. When an HRV-based model is built, appropriate HRV features should be selected because multiple HRV features can be simultaneously extracted in typical HRV analysis; however, the input of the proposed method is RRI data only. Thus, the proposed method does not require feature selection. In addition, the proposed method improved the performance, particularly the FP rate in comparison with the conventional HRV-based method; the sensitivity and the FP rate of the conventional HRV-based method were 91% and 1.7 times per hour, respectively.

Camera-based drowsiness detection methods achieved accuracies of 70%-90% [5], which are slightly better than the proposed method; however, most of them use facial expression evaluation by referees or subjective evaluation by questionnaires instead of EEG-based sleep scoring for driver sleepiness evaluation. Such an evaluation cannot detect sleep-related events observed in EEG only, such as SEM and microsleep. Thus, there is a possibility that previous studies overlooked sleep-related events and that the performance evaluation may have been inadequate.

In this experiment, the participants were required to attach some electrodes for ECG measurement on the skin before driving because ECG was measured with the EEG interface to measure EEG and ECG simultaneously. Although it is burdensome for drivers to attach electrodes in real driving, easy-to-wear ECG devices are currently available for use. For example, wearable textile electrodes using conductive fibers and smart shirts into which textile electrodes are woven have been developed for ECG measurement [48], [49]. Arquilla *et al.* demonstrated that there was no significant difference in the R wave detection accuracy between the conventional ECG electrodes and the textile electrodes [48]. Patch-typed ECG sensors also have been developed [50], [51]. VitalPatch (VitalConnect Inc., USA), which is an FDA-cleared, patch-typed commercial device, has already been used for Out-Of-Hospital clinical trials [52]. Thus, these easy-to-wear wearable devices can be used with the proposed method in real driving because the input of the proposed method is the RRI data only, and other signals are not needed.

The proposed method is not limited to drowsy driving and may be applied to drowsiness detection in other situations, such as working in an office because it requires only RRI data for detecting drowsiness.

The achievable drowsiness detection performance in other situations might be limited due to the low quality of ECG data. In the experiment, significant motion artifacts in RRI data rarely occurred since drivers did not move significantly. We will try the proposed method in various situations to confirm its applicability in situations other than driving.

Based on the foregoing, it is concluded that the proposed drowsiness detection method combining RRI data and SA-AE is more promising than conventional methods with respect to accuracy as well as practical use.

VI. Conclusion and Future Work

An RRI-based driver drowsiness detection method utilizing an anomaly detection algorithm has been proposed. In the proposed method, abnormal changes in the RRI data caused by drowsiness are detected by means of a self-attention autoencoder. The experimental results showed that 16 out of 18 sleep-related events during driving were correctly detected (sensitivity of 89 %), and the false-positive rate was 0.60 times per hour.

Limitations of the study come from the characteristics of the experimental data, i.e., the laboratory environment was highly controlled, the number of participants was limited, all participants were young Japanese persons, and the data were collected under a well-controlled experimental environment. Additional studies are required to confirm our results, in particular, whether alarms occur due to factors other than driver drowsiness or not, by using well-matched groups of participants in a real driving environment.

In future works, additional experimental data will be collected in order to improve the performance of the drowsiness detection model, which will be tested in a real driving environment. In addition, the proposed drowsiness detection method will be applied in other fields, such as office workers.

References

[1] S. G. Klauer, et al. The impact of driver inattention on near-crash/crash risk: An analysis using the 100-car naturalistic driving study data. *National Highway Traffic Safety Administration*, 2006.

[2] Fu-Chang Lin, Li-Wei Ko, Chun-Hsiang Chuang, Tung-Ping Su, and Chin-Teng Lin. Generalized eeg-based drowsiness prediction system by using a self-organizing neural fuzzy system. *IEEE Transactions on Circuits and Systems I: Regular Papers*, Vol. 59, No. 9, pp. 2044–2055, 2012.

[3] A. Hashemi, et al. Time driver's drowsiness detection by processing the eeg signals stimulated with external flickering light. *Basic Clin. Neurosci.*, Vol. 5, No. 1, pp. 22–27, 2014.

[4] M. H. Kryger, T. Roth, and W. C. Dement. *Principles and practice of sleep medicine*. Elsevier Inc., 6th edition, 2017.

[5] S. Kaplan. Driver behavior analysis for safe driving: A survey. *IEEE Trans. Intell. Transp. Syst.*, Vol. 16, No. 6, pp. 3017–3032, 2015.

[6] R. O. Mbouna, et al. Visual analysis of eye state and head pose for driver alertness monitoring. *IEEE Trans. Intell. Transp. Syst.*, Vol. 14, No. 3, pp. 1462–1469, 2013.

[7] J. Jo, et al. Detecting driver drowsiness using feature-level fusion and user-specific classification. *Expert Syst. Appl.*, Vol. 41, No. 4, pp. 1139–1152, 2014.

[8] J. Trinder, et al. Autonomic activity during human sleep as a function of time and sleep stage. *J. Sleep Res.*, Vol. 10, No. 4, pp. 253–264, 2001.

[9] K. T. Chui, et al. An accurate ecg-based transportation safety drowsiness detection scheme. *IEEE Trans. Ind. Informat.*, Vol. 12, No. 4, pp. 1438–1452, 2016.

[10] B.-G. Lee, et al. Real-time physiological and vision monitoring of vehicle driver for non-intrusive drowsiness detection. *IET Commun.*, Vol. 5, No. 17, pp. 2461–2469, 2011.

[11] Marek Malik, J Thomas Bigger, A John Camm, Robert E Kleiger, Alberto Malliani, Arthur J Moss, and Peter J Schwartz. Heart rate variability: Standards of measurement, physiological interpretation, and clinical use. *European heart journal*, Vol. 17, No. 3, pp. 354–381, 1996.

[12] A. Malliani, M. Pagani, F. Lombardi, and S. Cerutti. Cardiovascular neural regulation explored in the frequency domain. *Circulation*, Vol. 84, No. 2, pp. 482–492, 1991.

[13] Koichi Fujiwara, Miho Miyajima, Toshitaka Yamakawa, Erika Abe, Yoko Suzuki, Yuriko Sawada, Manabu Kano, Taketoshi Maehara, Katsuya Ohta, Taeko Sasai-Sakuma, Tetsuo Sasano, Masato Matsuura, and Eisuke Matsushima. Epileptic seizure prediction based on multivariate statistical process control of heart rate variability features. *IEEE Transactions on Biomedical Engineering*, Vol. 63, No. 6, pp. 1321–1332, June 2016.

[14] Toshitaka Yamakawa, Miho Miyajima, Koichi Fujiwara, Manabu Kano, Yoko Suzuki, Yutaka Watanabe, Satsuki Watanabe, Tohru Hoshida, Motoki Inaji, and Taketoshi Maehara. Wearable epileptic seizure prediction system with machine-learning-based anomaly detection of heart rate variability. *Sensors*, Vol. 20, No. 14, 2020.

[15] C. Nakayama, K. Fujiwara, Y. Sumi, M. Matsuo, M. Kano, and H. Kadotani. Application of artificial intelligence to obstructive sleep apnea screening using heart rate variability analysis. *Physiol. Meas*, Vol. 40, No. 12, p. 5001, 2019.

[16] Ayako Iwasaki, Chikao Nakayama, Koichi Fujiwara, Yukiyoshi Sumi, Masahiro Matsuo, Manabu Kano, and Hiroshi Kadotani. Screening of sleep apnea based on heart rate variability and long short-term memory. *Sleep and Breathing*, Vol. 25, pp. 1821–1829, 2021.

[17] F. Versace, M. Mozzato, G. De Min Tona, C. Cavallero, and L. Stegagno. Heart rate variability during sleep as a function of the sleep cycle. *Biol Psychol*, Vol. 63, No. 2, pp. 146–162, 2003.

[18] Mohsen Babaeian, K. Amal Francis, Khalil Dajani, and Mohammad Mozumdar. Real-time driver drowsiness detection using wavelet transform and ensemble logistic regression. *International Journal of Intelligent Transportation Systems Research*, Vol. 17, No. 3, pp. 212–222, 2019.

[19] J. Vicente, P. Laguna, A. Bartra, and R. Bailón. Drowsiness detection using heart rate variability. *Med Biol Eng Comput*, Vol. 54, No. 6, pp. 927–937, 2016.

[20] N. Ito, S. Minusa, T. Tanaka, Y. Li, and H. Kuriyama. Prediction of future collision risk using the time-series autonomic nerve function recorded during driving. *IEEE Access*, 2023.

[21] Koichi Fujiwara, Erika Abe, Keisuke Kamata, Chikao Nakayama, Yoko Suzuki, Toshitaka Yamakawa, Toshihiro Hiraoka, Manabu Kano, Yukiyoshi Sumi, Fumi Masuda, Masahiro Matsuo, and Hiroshi Kadotani. Heart Rate Variability-Based Driver Drowsiness Detection and Its Validation With EEG. *IEEE Transactions on Biomedical Engineering*, Vol. 66, No. 6, pp. 1769–1778, 2019.

[22] Ashish Vaswani, Noam Shazeer, Niki Parmar, Jakob Uszkoreit, Llion Jones, Aidan N. Gomez, Łukasz Kaiser, and Illia Polosukhin. Attention is all you need. *Advances in Neural Information Processing Systems*, Vol. 2017-Decem, No. Nips, pp. 5999–6009, 2017.

[23] G. E. Hinton and R. R Salakhutdinov. Reducing the dimensionality of data with neural networks. *Science*, Vol. 313, No. 5786, pp. 504–507, 2006.

[24] K. Iwamoto, K Hori, K. Fujiwara, and M. Kano. Real-driving-implementable drowsy driving detection method using heart rate variability based on long short-term memory and autoencoder. In *IFAC BMS 2021*. Ghent, Belgium, Sept. 19-22 2021.

[25] U. J. Ilg. Slow eye movements. *Prog Neurobiol*, Vol. 53, No. 3, pp. 293–329, 1997.

[26] American Academy of Sleep Medicine. *International Classification of Sleep Disorders*.

[27] American Academy of Sleep Medicine. *The AASM Manual for the Scoring of Sleep and Associated Events: Rules, Terminology and Technical Specifications*, version 2.3 edition, 2016.

[28] F. Jurysta, et al. A study of the dynamic interactions between sleep eeg and heart rate variability in healthy young men. *Clin. Neurophysiol.*, Vol. 114, No. 11, pp. 2146–2155, 2003.

[29] S. L. Wendt, P. Welinder, H. B. Sorensen, P. E. Peppard, P. Jennum, P. Perona, E. Mignot, and S. C. Warby. Inter-expert and intra-expert reliability in sleep spindle scoring. *Clin Neurophysiol*, Vol. 126, No. 8, pp. 1548–1556, 2015.

[30] E. Abe, K. Fujiwara, T. Hiraoka, T. Yamakawa, and M. Kano. Development of drowsiness detection method by integrating heart rate variability analysis and multivariate statistical process control. *SICE JCMSI*, Vol. 9, No. 1, pp. 10–17, 2016.

[31] J. F. MacGregor and T. Kourti. Statistical process control of multivariate processes. *Control Eng. Pract.*, Vol. 3, pp. 403–414, 1995.

[32] M. Kano, et al. A new multivariate statistical process monitoring method using principal component analysis. *Comput. Chem. Engng.*, Vol. 25, No. 7-8, pp. 1103–1113, 2001.

[33] Tomonobu Kodama, Keisuke Kamata, Koichi Fujiwara, Manabu Kano, Toshitaka Yamakawa, Ichiro Yuki, and Yuichi Murayama. Ischemic stroke detection by analyzing heart rate variability in rat middle cerebral artery occlusion model. *IEEE Transactions on Neural Systems and Rehabilitation Engineering*, Vol. 26, No. 6, pp. 1152–1160, 2018.

[34] Juan Bolea, Esther Pueyo, Michele Orini, and Raquel Bailón. Influence of heart rate in non-linear hrv indices as a sampling rate effect evaluated on supine and standing. *Frontiers in Physiology*, Vol. 7, p. 501, 2016.

[35] Sebastian J. Wetzel. Unsupervised learning of phase transitions: From principal component analysis to variational autoencoders. *Phys. Rev. E*, Vol. 96, p. 022140, 2017.
[36] Mark A. Kramer. Nonlinear principal component analysis using autoassociative neural networks. *AIChE Journal*, Vol. 37, No. 2, pp. 233–243, 1991.
[37] Zhouhan Lin, Minwei Feng, Cicero Nogueira Dos Santos, Mo Yu, Bing Xiang, Bowen Zhou, and Yoshua Bengio. A structured self-attentive sentence embedding. *5th International Conference on Learning Representations, ICLR 2017 - Conference Track Proceedings*, pp. 1–15, 2017.
[38] Kaiming He, Xiangyu Zhang, Shaoqing Ren, and Jian Sun. Deep residual learning for image recognition. In *Proceedings of the IEEE Conference on Computer Vision and Pattern Recognition (CVPR)*, June 2016.
[39] M. W. Johns. A new method for measuring daytime sleepiness : the epworth sleepiness scale. *Sleep*, Vol. 14, No. 6, pp. 540–545, 1991.
[40] K. Kroenke, R. L. Spitzer, and J. B. Williams. The PHQ-9: validity of a brief depression severity measure. *J Gen Intern Med*, Vol. 16, No. 9, pp. 606–613, 2001.
[41] L. D. Rosenthal and D. C. Dolan. The Epworth sleepiness scale in the identification of obstructive sleep apnea. *J Nerv Ment Dis*, Vol. 196, No. 5, pp. 429–431, 2008.
[42] Alex Sherstinsky. Fundamentals of recurrent neural network (rnn) and long short-term memory (lstm) network. *Physica D: Nonlinear Phenomena*, Vol. 404, p. 132306, 2020.
[43] K. K. Gulia and V. M. Kumar. Sleep disorders in the elderly: a growing challenge. *Psychogeriatrics*, Vol. 18, No. 3, pp. 155–165, 2018.
[44] J. L. Rodgers, J. Jones, S. I. Bolleddu, S. Vanthenapalli, L. E. Rodgers, K. Shah, K. Karia, and S. K. Panguluri. Cardiovascular Risks Associated with Gender and Aging. *J Cardiovasc Dev Dis*, Vol. 6, No. 2, 2019.
[45] E. Tobaldini, L. Nobili, S. Strada, K. R. Casali, A. Braghiroli, and N. Montano. Heart rate variability in normal and pathological sleep. *Front Physiol*, Vol. 4, p. 294, 2013.
[46] K. J. Finkel, A. C. Searleman, H. Tymkew, C. Y. Tanaka, L. Saager, E. Safer-Zadeh, M. Bottros, J. A. Selvidge, E. Jacobsohn, D. Pulley, S. Duntley, C. Becker, and M. S. Avidan. Prevalence of undiagnosed obstructive sleep apnea among adult surgical patients in an academic medical center. *Sleep Med*, Vol. 10, No. 7, pp. 753–758, 2009.
[47] Task Force of The European Society of Cardiology and The North American Society of Pacing and Electrophysiology. Guidelines heart rate variability - standards of measurement, physiological interpretation, and clinical use. *Eur. Heart J.*, Vol. 115, No. 5, pp. 354–381, 1996.
[48] K. Arquilla, A. K. Webb, and A. P. Anderson. Textile Electrocardiogram (ECG) Electrodes for Wearable Health Monitoring. *Sensors (Basel)*, Vol. 20, No. 4, 2020.
[49] A. B. Nigusse, D. A. Mengistie, B. Malengier, G. B. Tseghai, and L. V. Langenhove. Wearable Smart Textiles for Long-Term Electrocardiography Monitoring-A Review. *Sensors*, Vol. 21, No. 12, 2021.
[50] Meina Li and Youn Tae Kim. Development of patch-type sensor module for wireless monitoring of heart rate and movement index. *Sensors and Actuators A: Physical*, Vol. 173, No. 1, pp. 277–283, 2012.
[51] Mohammad Zulqarnain, Stefano Stanzione, Ganesh Rathinavel, Steve Smout, Myriam Willegems, Kris Myny, and Eugenio Cantatore. A flexible ecg patch compatible with nfc rf communication. *npj Flexible Electronics*, Vol. 4, No. 1, p. 13, 2020.
[52] D. M. Levine, K. Ouchi, B. Blanchfield, A. Saenz, K. Burke, M. Paz, K. Diamond, C. T. Pu, and J. L. Schnipper. Hospital-Level Care at Home for Acutely Ill Adults: A Randomized Controlled Trial. *Ann Intern Med*, Vol. 172, No. 2, pp. 77–85, 2020.